ANAS Transactions Earth Sciences 1 / 2026

http://www.journalesgia.com

ELECTRICAL RESISTIVITY SURVEY AND THE NEAR-SURFACE STRUCTURE EXPLORATION OF THE SHIKHZAHIRLI MUD VOLCANO (AZERBAIJAN)

Kadirov F.A.[1,2,3], Salamov A.M.[1], Safarov R.T.[1,2]*, Najafov O.F.[1], Samadli P.M.[2], Mammadov S.G.[1], Zamanova A.H.[1,2]

[1]Ministry of Science and Education of the Republic of Azerbaijan, Institute of Geology and Geophysics, Azerbaijan
119 H. Javid Ave., Baku, AZ1073
[2]Ministry of Science and Education of the Republic of Azerbaijan, Institute of Oil and Gas, Azerbaijan
9, F.Amirov str., Baku, AZ1000
[3]Faculty of Geology, Baku State University, Azerbaijan
33, Acad. Zahid Khalilov str., Baku AZ 1148
**Corresponding author: rafiqsafarov@gmail.com*

Keywords: *mud volcano, eruption, vertical electrical sounding, resistivity, geoelectrical section, Shikhzahirli, fault*

Summary. Mud volcanism is widespread in Azerbaijan, with over 300 land- and offshore mud volcanoes. These volcanoes are associated with oil and gas fields, and many of them are currently active. The Shikhzahirli mud volcano is located west-northwest of Baku, in the Shamakhi-Gobustan region, and is one of the world's active mud volcanoes. From 1844 to 2025, there were approximately 25 major eruptions. The last volcano eruption occurred on January 9, 2021 in three phases. The longest was the third phase, which lasted 7 minutes. Geoelectrical measurements, consisting of the vertical electrical sounding (VES) method, were performed for the first time in the Shikhzahirli mud volcano occurrence, aiming to evaluate the near-surface mud chambers, as well as to track the feeder channel. The VES measurements indicate that within the first 50 m below ground surface, no shallow-depth accumulation chambers occurred. The eruption triggered by gas accumulation appears to branch in the near-surface region; in one location, the upward migration path is almost vertical, whereas in others it is slanted. As a result of investigations, it was found that the volcano most likely has two vents located at the hinge of an anticline. The rocks in the geological section of the study area have been found to have relatively high moisture content. The probable thickness of the volcanic breccia is estimated to be consistent with the depth of the bedrock surface, which ranges from 135 to 150 m. Proposed multidirectional faults, presumably formed because of a mud volcano eruption, were identified.

Introduction

Mud volcanism is widespread in Azerbaijan: there are over 300 mud volcanoes (Aliyev et al., 2015; Yakubov et al., 1971) on land and offshore. These volcanoes are associated with oil and gas fields, and most of them are currently active. The Shikhzahirli mud volcano located in the Shamakhi-Gobustan region is one of the most active volcanoes in the world (Aliyev, Bayramov, 1999, 2000; Alizadeh et al., 2016; Kokh et al., 2017). From 1844 to 2025, there were approximately 25 major eruptions. The location map of the Shikhzahirli mud volcano and effusion of volcanic breccia are shown in Fig. 1 and Fig. 2, respectively.

Mud volcanoes observed in Azerbaijan pose serious problems due to the negative consequences they cause, but since they are unstable and unpredictable phenomena, it is highly desirable to better understand their activity to prevent possible casualties: large mud flows and flames that can sometimes accompany an eruption.

Since the Shikhzahirli mud volcano is one of the active volcanoes and is unique in terms of the large volume of erupted mud flow and the composition of emitted gases, it is necessary to study its area in detail using deep geophysical measurements.

The aim of this study is to investigate the electrical properties and trace the feeder channel of the Shikhzahirli mud volcano using geoelectrical survey (vertical electrical sounding, VES) (Fig.1).

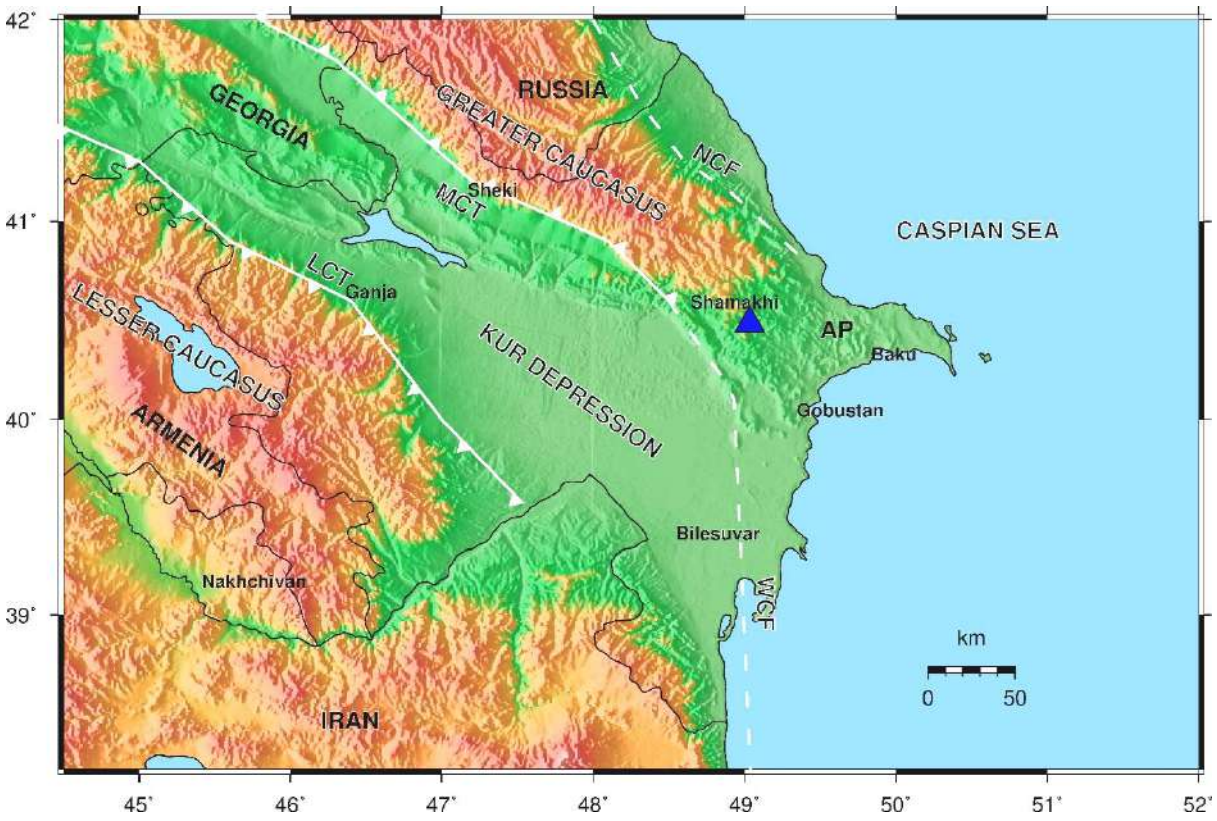

Fig. 1. The location of the Shikhzahirli mud volcano (blue triangle).
AP – The Absheron peninsula, NCF – The North Caspian Fault, MCT – The Main Caucasus Thrust, LCT – The Lesser Caucasus Thrust, WCF – The West Caspian Fault

Fig. 2. The Shikhzahirli mud volcano. Effusion of volcanic breccia (Aliyev, Yetirmishli, 2021)

Geological and geodynamic background

The Shikhzahirli mud volcano is located in the Shamakhi-Gobustan depression zone of Azerbaijan. The deepest eastern part of the Shamakhi-Gobustan depression, filled with shallow-water Pliocene sediments, merges with an area of the same sediments on the Absheron Peninsula and, together with the latter, forms the Absheron-Gobustan periclinal depression, which forms the northwestern rim of the vast and deep South Caspian Basin (Khain, 1984).

In Gobustan, it is distinguished by the development of the Paleogene and Miocene deposits at the

surface and by the almost strictly latitudinal orientation of its folds with isoclinal and even imbricated structures. The Absheron deposits are widespread in the Shamakhi-Gobustan region. They contribute to the construction of structural units of various shapes and are dislocated with varying degrees of intensity.

Most mud volcanoes are concentrated in areas that experienced prolonged subsidence not only during the Quaternary but also during previous geological periods: the Lower Kur Depression, the Absheron Pericline and Shamakhi-Gobustan Foredeep, and the South Caspian Basin. Mud volcanoes are widespread in all these depression zones, indicating strong manifestations of oscillatory, folding, and faulting movements during the Anthropogenic period (Kadirov, Mukhtarov, 2004). The primary cause of mud volcanism was negative oscillatory movements combined with folding and faulting movements (Ali-Zade, 1987; Kadirov et al., 2005). A geological map of the Shikhzahirli mud volcano area is shown in Fig. 3.

Figure 4 illustrates the velocity data for global positioning system (GPS) sites within the area encompassing the western and southern shores of the South Caspian Sea along with the distribution of mud volcanoes (Kadirov et al., 2008; Kadirov, Safarov, 2013; Kadirov et al., 2014, 2024).

On a large scale, the GPS velocity field shows the northeastward motion of the Caucasus region and its neighboring areas relative to Eurasia, south of the Main Caucasus Thrust Fault (MCT). It is noteworthy that significant reductions in site velocities and clockwise rotation are observed between sites west of the West Caspian Fault (WCF) in the Kur Depression and Talish region, and sites located to the east of the WCF within the Absheron Peninsula. The observed decrease and disparity in GPS vector directions indicate elevated strain accumulation rates of approximately 6 millimeters per year in the southern direction towards the Absheron Peninsula. Furthermore, GPS-derived motions on the northern slope of the Greater Caucasus and along the Caspian coast in Azerbaijan north of the Absheron Peninsula suggest the presence of south-dipping thrust faulting along the North Caucasus. This thrust faulting is characterised by a southward inclination within the Absheron Peninsula and continues inland from the Caspian coast, traversing the peninsula in a westerly direction before terminating at the Caspian Sea.

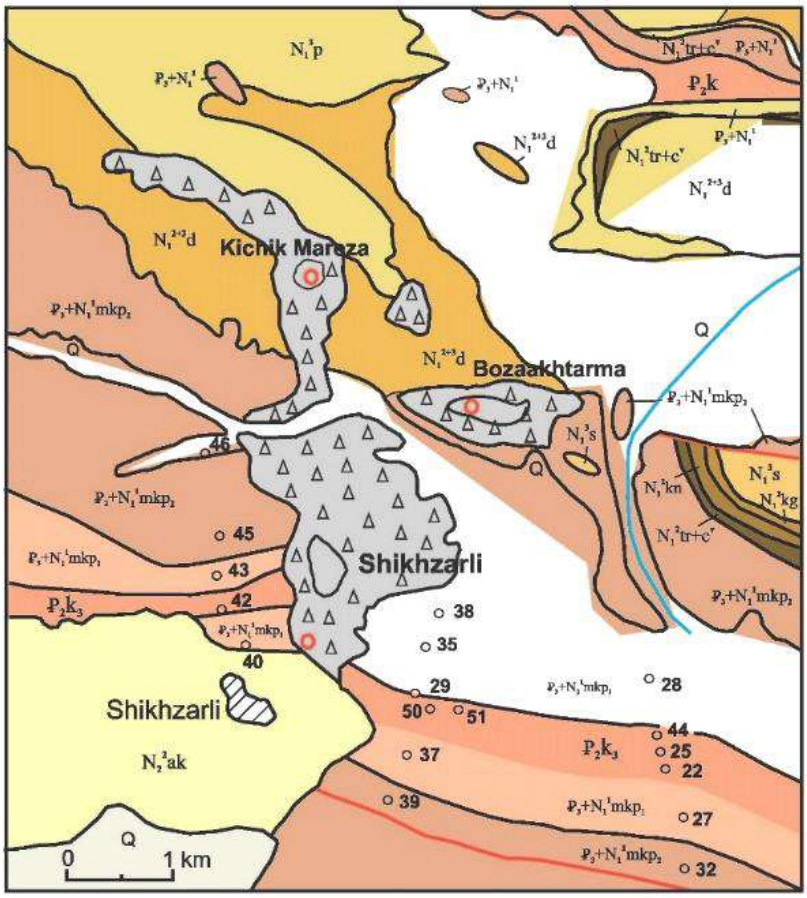

Fig. 3. Geological map of Shikhzahirli mud volcano location area (Aliyev et al., 2015)

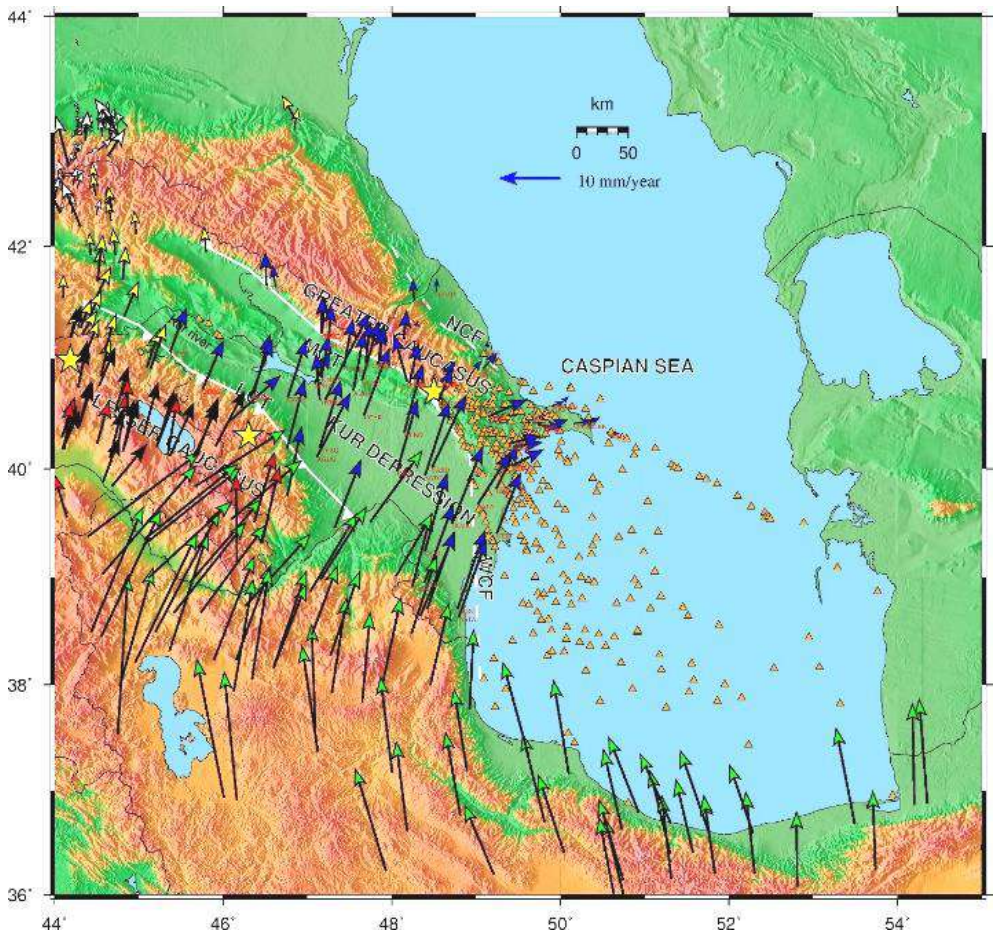

Fig. 4. GPS velocities with respect to Eurasia for the eastern AR-EU collision zone. Yellow stars show 1139, M7.3 Ganja; 1902, M6.9 Shamakhi; 1988, M6.8 Spitak and 1991, M7.0 Racha earthquake epicenters. Blue arrows indicate Azerbaijan GPS sites (Kadirov et al., 2024), green arrows stand for the Iranian GPS sites (Raeesi et al., 2017), Red arrows show the Armenian GPS sites (Karakhanyan et al., 2013), Yellow arrows demonstrate Georgian GPS sites (Sokhadze et al., 2018), White arrows display the Russian GPS sites (Milyukov et al., 2015), Black arrows are velocities from Reilinger et al., (2006). Orange triangles show the mud volcanoes.

Furthermore, the GPS vectors in the region, specifically in the Absheron Peninsula and along the western Caspian coast, exhibit a pronounced eastward motion. This eastward shift is interpreted as the result of a left-lateral strike-slip mechanism acting within this segment of the fault.

Contractions are observed in the Greater Caucasus, Gobustan, the Kur Depression, the Nakhchivan Autonomous Republic, and the areas bordering Iran. The contraction axes show that crustal shortening in the Greater Caucasus region occurs in a northeasterly direction, with the shortening in the Shamakhi region (MEDR) being nearly submeridional. The deformation rate between the KURD (Kurdemir) and MEDR (Madrasa) GPS points is ~16 x 10^{-8}/yr.

Geophysical surveys. Methodology and interpretation of field work

As noted above, comprehensive field geophysical surveys were conducted along five profiles by the electrical prospecting method using a four-electrode symmetrical AMNB array.

It should be noted that electrical prospecting using the vertical electrical sounding (VES) method was conducted in this area for the first time.

As it is well known, the modern VES theory is based on the Schlumberger mathematical model. It allows calculating the apparent electrical resistivity (ρ_a) of a multilayer medium with horizontal interfaces, depending on the specific electrical resistivity (ρ_s), the thickness of the individual layers, and the size of the VES survey setup. However, using this model precludes the possibility of a definitive solution to the inverse problem – determining the depth of horizontal interfaces and the specific electrical resistivity of individual layers from a set of ρ_a values obtained during measurements with different setups (Lowrıe, 2007; Griffiths, King, 1981; Keller, Frischknecht, 1966).

This goal can be mostly achieved by constructing a new model based on the following simplifying assumptions on the characteristics of the current distribution in a flat-layered medium when placing electrodes on the daylight surface:

– the measured ρ_a value characterises the geological section to a certain depth H, which is entirely determined by the ratio between the dimensions of potential (MN) and the feeder (AB) lines, and when MN<<AB the value of H is AB/2 (in practice, MN should be no more than 0.1 AB);

– the ρ_a value is determined only by the vertical component of the current density, i.e., it represents a certain averaged electrical characteristic of the medium in the vertical direction, depending on the specific electrical resistances ρ_{si} of each layer, and the "contribution" to the value of ρ_a of each ρ_{si} depends on the thickness of the given layer h_i.

The adopted assumptions allow constructing the following simple formula, which establishes a correspondence between the set of values (ρ_{si}, h_i) of the n-layer section and the value of ρ_a:

$$\rho_a = \frac{\rho_1 h_1 + \rho_2 h_2 + \cdots + \rho_{si} h_i}{h_1 + h_2 + \cdots h_i} = \frac{\sum_{i=1}^{n} \rho_{si} h_i}{\sum_{i=1}^{n} h_i} \quad (1)$$

where, $\sum_{i=1}^{n} h_i$, $m=h_i$, m is the depth of the n-th layer base.

Since, according to the accepted assumption, the value of h_i is completely determined by the relationship between MN and AB, and therefore, formula (1) can be used to solve the inverse problem of determining the parameters of a geoelectric section from a set of ρ_a values obtained with different sizes of the survey setup. Indeed, given a series of successive ρ_{ai} values and h_i (i = 1, 2, ... n), one can sequentially determine h_i and ρ_{si}, i.e., the thickness and specific resistivity of each layer.

This means that for any i-th layer $h_i = h_i - h_{i-1}$ or $h_i = (AB/2)_i - (AB/2)_{i-1}$ (2)

To calculate the apparent electrical resistivity ρ_a, the formula

$$\rho_a = K_{VES} * \Delta U_{mV} / I_{mA} \quad (3)$$

was used (Yakubovski, Renard, 1991).

And to determine the specific electrical resistivity of individual layers, formula (4) is used, when $\rho_{ai} > \rho_{ai-1}$. (Popov et al., 1990; Galin, 1989)

$$\rho_{si} = \left[\rho_{ai} * \left(\frac{AB}{2}\right)_i - \rho_{ai-1} * \left(\frac{AB}{2}\right)_{i-1}\right] / \left[\left(\frac{AB}{2}\right)_i - \left(\frac{AB}{2}\right)_{i-1}\right] \quad (4)$$

and in the case $\rho_{ai-1} > \rho_{ai}$ the formula

$$\rho_{si} = \left\{\left[\left(\frac{AB}{2}\right)_i - \left(\frac{AB}{2}\right)_{i-1}\right] * \rho_{ai-1} * \rho_{ai}\right\} / \left[\rho_{ai-1} * \left(\frac{AB}{2}\right)_i - \rho_{ai} * \left(\frac{AB}{2}\right)_{i-1}\right] \quad (5)$$

(Salamov et al., 2015) is used.

Expressions (2), (3), and (4) are the main calculation formulas in the proposed method for determining the parameters of the geoelectric section based on VES data for installations with MN<<AB.

As follows from formulas (2), (4), and (5), the proposed model enables determination of the thickness and specific electrical resistivity of any layer, regardless of the parameters of the overlying layer.

Taking into account the above, for the purpose of detailed dissection of the geological section and more accurate depth determination of the individual lithological varieties, as a result of experimental measurements carried out using the VES method, the sizes of the feeder line AB/2 and the receiver line MN/2 were adopted, respectively: AB/2 =1; 2; 3; 4; 5; 6; 7; 8; 9; 10,10; 12,12; 14; 16; 18; 20; 22; 24,24; 26,26; 28; 30; 32; 34; 36,36; 38,38; 40,40; 42; 44; 46; 48; 50,50; 52; 54; 56; 58; 60; 63; 66; 69; 72,72; 75,75; 78; 81; 84; 87; 90,90; 93,93; 96; 99; 102; 105; 108; 111; 114; 117; 120; 125,125; 130,130; 135, 140; 145; 150; 155; 160; 165; 170; 175; 180; 185; 190; 195; 200 and MN/2=0,3; 0,3; 0,3; 0,3; 0,3; 0,3; 0,3; 0,3; 0,3; 0,3; 0,3; 0,3; 1; 0,3; 1; 1; 1; 1; 1,2; 1,2; 2, 2, 2, 2; 2,3; 2,3; 2,3; 3; 3; 3; 3; 3,5; 3,5; 5; 5; 5; 5; 5; 5; 5; 5,7; 5,7; 7; 7; 7; 7; 7,9; 7,9; 9; 9; 9; 9; 9; 9; 9; 9; 9; 9,12; 9,12; 12; 12; 12; 12; 12; 12; 12; 12; 12; 12; 12; 12; 12; 12; 12; 12; 12,15 (Salamov et al., 2025).

Increasing the number of measurements at a single observation point made it possible to identify thin layers in the geological section of the study area (Popov et al., 1990; Galin, 1989; Salamov et al., 2015, 2023, 2025).

The profile directions were northeast, southwest, and east-west (Fig. 5).

For field measurements, ERA-MAX electrical prospecting equipment operating at 4.88 Hz was used.

Results and Discussion

Geophysical field surveys using the VES method were conducted in the Shikhzahirli mud volcano area. These measurements determined the apparent electrical resistivity of rocks within the geological section across the area and to a depth of 200 meters. The resulting apparent electrical resistivity values were interpreted, and the specific electrical resistivity of rocks was determined (Fig. 6).

Based on the apparent and specific electrical resistivity values, corresponding sections were constructed along 5 profiles (I-I, II-II, III-III, IV-IV, V-V). These are the vertical sections based on apparent electrical resistivity values, and the supposed lithological-geophysical sections based on specific electrical resistivity values.

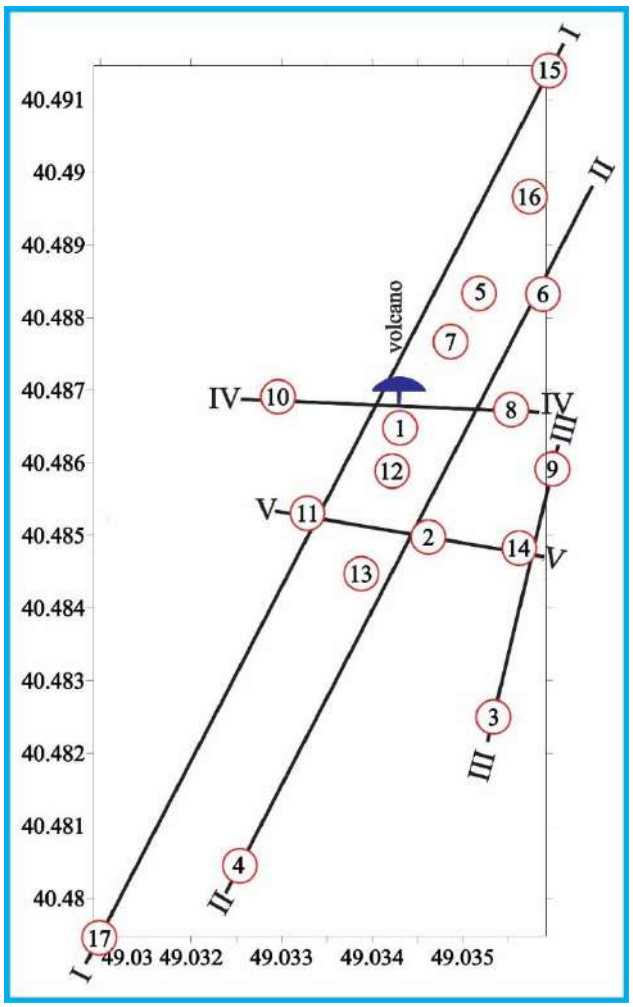

Fig. 5. Layout of geophysical profiles

1 – geophysical profile lines; 2 – VES points

According to the profile I-I section constructed, it is evident that, up to a depth of 200 m, the apparent electrical resistivity (ρa) of rocks varies between 1 and 18, while the specific electrical resistivity (ρs) changes from 0.5 to 14 Ohm-m (Fig. 6).

Approximately eight layers of varying thicknesses, approximately 15–20 m, are traced to the studied depth, indicating the duration of the eruption. The specific electrical resistivity ρ_s of these layers varies between 4 and 14 Ω · m.

In the section the thickness of identified layers is almost similar and has a relatively plain bedding and are placatively deformed. This suggests that these layers formed during a prolonged mud volcano eruption in a marine environment. The catalog indicates that the Shikhzahirli mud volcano has erupted 24 times, excluding marine eruptions. However, the data obtained from geophysical surveys refute this information. In general, it is necessary to clarify what a volcanic eruption is and can minor volcanic activity be called an eruption?

The top of the bedrock layers was identified at a depth of approximately 135-150 m, and their ρ_s values range from 12 to 14 Ohm-m.

The bedrock layers are intersected by faults in different directions.

The mud volcano vent is believed to lie within the interval of the VES №1–11 survey points, in the hinge part of the anticline. The centerline of this structure has an arcuate outline. In the area of VES №13–16 survey points, eruption material (slurry) with ρ_s of 0.5–3.0 Ohm-m is accumulated, forming a mushroom-shaped vent, which is typical of mud volcanoes.

To trace the areal and depth distribution of rocks using the averaged values of ρ_a and ρ_s, corresponding maps were constructed (Fig. 7).

On the ρ_a map, from north to south, rocks with different types are observed. In the northern part of the area, ρ_a values change between 4.5-6.0 Ohm-m, while in the central part of the study area, a lineage of rocks in a northeast-southwest direction with low ρ_a values of 3.3-4.5 Ohm-m is observed. Finally, in the southern part, rocks with relatively high ρ_a values (4.5–9.0 Ohm m) are observed.

The volcanic vent area is characterised by very low ρ_a values, which are associated with the liquid material of the mud volcano.

On the ρ_s map, two distinct areas are distinguished based on specific electrical resistivity: a relatively high-resistivity area, where rock resistivity varies between 5 and 14 Ohm-m, developed in the northern and western parts of the area; and a low-resistivity area, encompassing the southeastern part of the area, where sediment resistivity varies between 0.3 and 4.8 Ohm-m (Fig. 7).

Analysis of the given maps suggests that the mud volcano area stands out from the rest of the area by having low electrical resistivity, which is natural.

Based on the average values of natural moisture content (W_r) and moisture content of rocks underwater (W_{rw}), corresponding maps were constructed (Fig. 8).

The purpose of compiling these maps was to thoroughly examine the areal and depth distributions of the supposed natural moisture content and the moisture content of underwater rocks.

The mud volcano area is conventionally divided into three parts based on natural moisture content. The northern part of the area is characterised by low natural moisture content W_r, varying between 22% - 28%, both in depth and area. In the central part, these indicators range from W_r = 28% to 34% (Fig. 8). In the southern part of the study area, natural moisture content increases significantly, reaching 50% and higher.

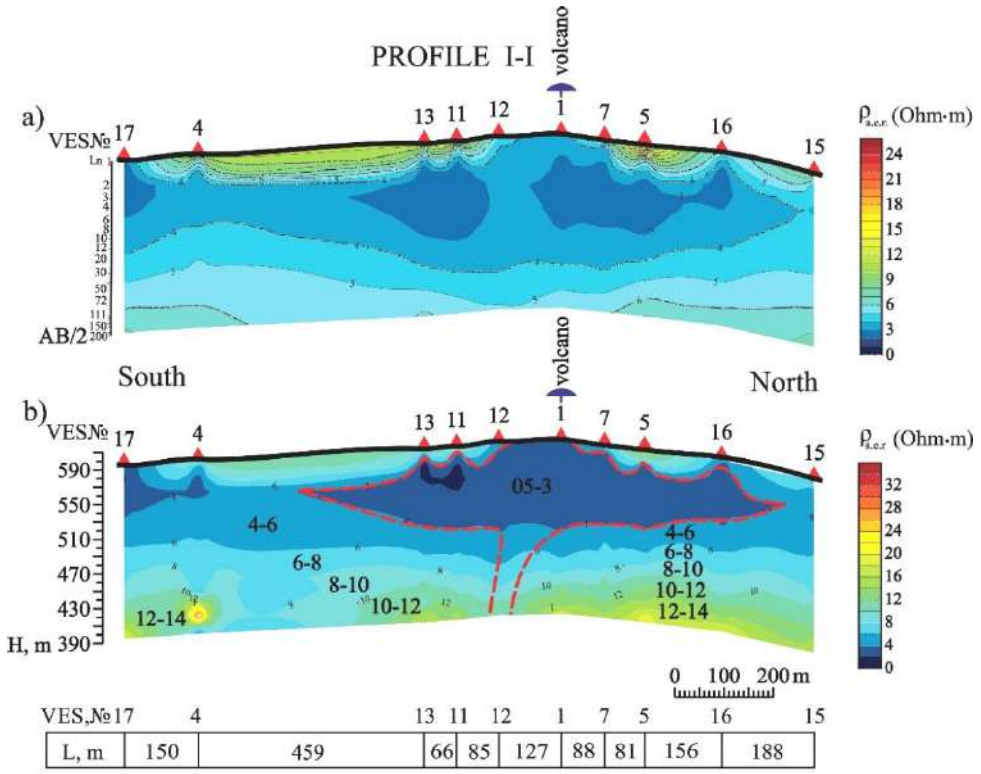

Fig. 6. Sections along profile I-I based on VES data: a – vertical section based on apparent electrical resistivity values of rocks; b – supposed lithological-geophysical section based on specific electrical resistivity values

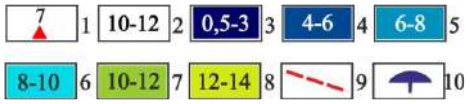

1 – VES points and their numbers; 2 – values of specific electrical resistivity of rocks; 3-8 – resistivity intervals; 9 – supposed faults identified by VES data; 10 – mud volcano crater

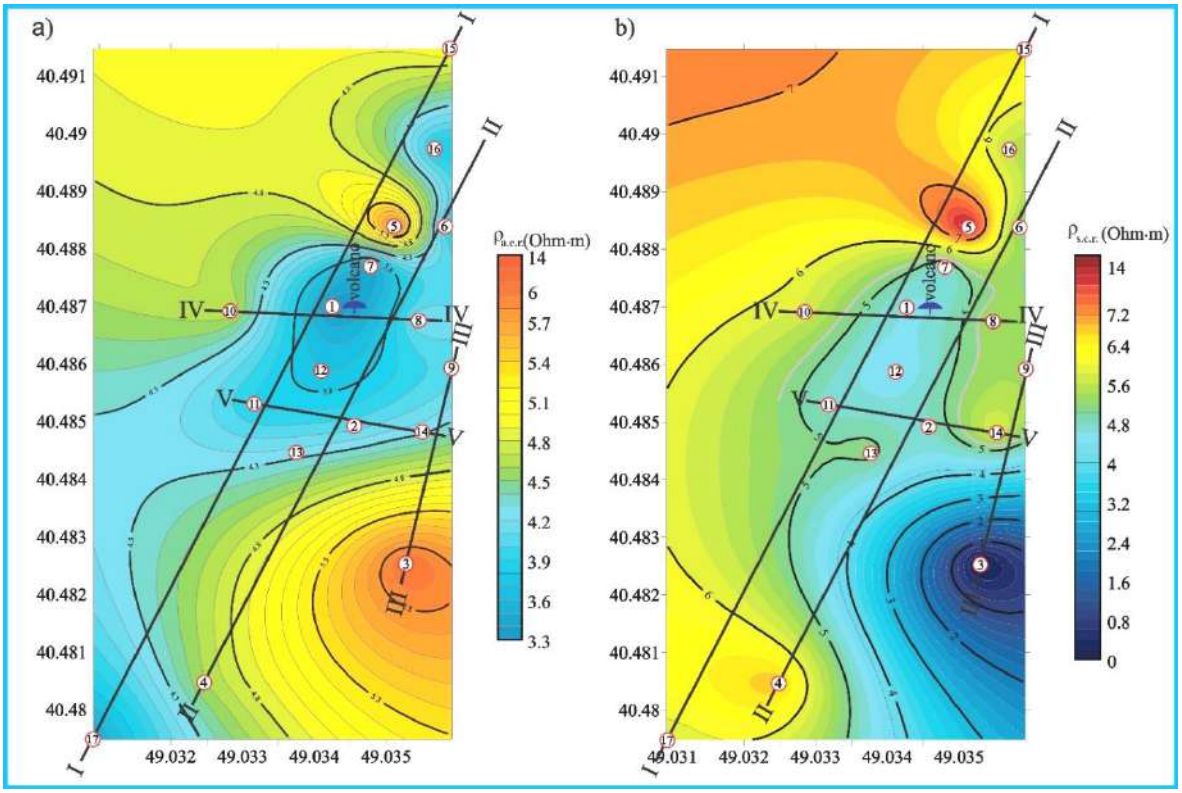

Fig. 7. Maps of ρ_a and ρ_s constructed based on VES data

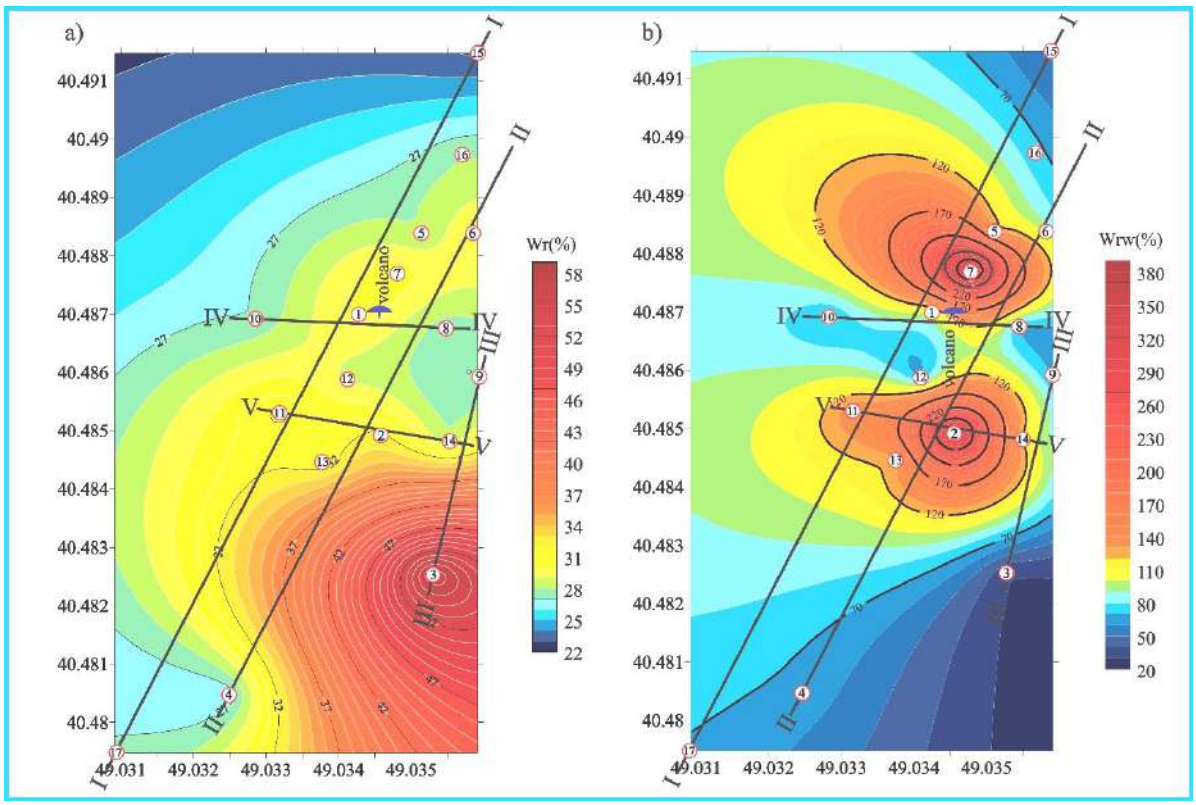

Fig. 8. W_r (a) and W_{rw} (b) maps constructed based on VES data

A moisture content map of the underwater rock revealed that the mud volcano presumably has two vents – one near VES №7 and the other near VES №2, which is a new finding.

In these areas, the data suggest that the rocks composing the geological section are in a substrate (slurry) state.

Based on VES geophysical survey data, rock densities were determined for the geological cross-section of the study area. As a result, maps of the supposed rock densities (a) and underwater rock densities (b) were constructed.

The purpose of these maps was to more precisely determine the area of the future mud volcano crater (Fig. 9).

According to the map of the supposed rock density V_r (Figure 9a), the study area is divided into three parts from south-east to north-west.

In the south-eastern part of the area, the rock density changes between 0.9-1.38 t/m^3, in the middle part of the area, rock densities along the stripe in north-east south-west direction varies in the range of 1.4-1.78 t/m^3, and finally, in the north-western part, these indicators vary within the range of 1.78-1.86 t/m^3.

The map of underwater rock densities also identifies three areas of varying rock density in the geological section.

In the southeastern part of the study area, underwater rocks have a specific weight of 0.89-0.96 t/m^3. In the central part of the area, a section with a low specific weight of 0.81-0.88 t/m^3 is identified.

It is assumed that the area with a low specific weight of underwater rocks is associated with both the liquid products of the mud volcano and atmospheric precipitation.

Based on the compiled map of underwater rock density, it can be assumed that the future crater of the mud volcano will be approximately bound by a line with a value of 0.88 t/m^3. It should be noted that the area of the future crater, at least, cannot be smaller than the outlined one.

Based on the average seismic acceleration, a section with low seismic acceleration is identified in the central part of the study area, coinciding with the vents of the mud volcano (Fig. 10a). The lowest seismic acceleration values are observed around VES №2, 11, and 13, which may be related to the second vent of the mud volcano.

The data obtained indicate that the mud volcano area is highly seismically active.

Faults in various directions were identified in the volcano crater. In other words, there is no correlation between fault directions. This suggests that these faults formed due to a mud volcano eruption (Fig. 10 b).

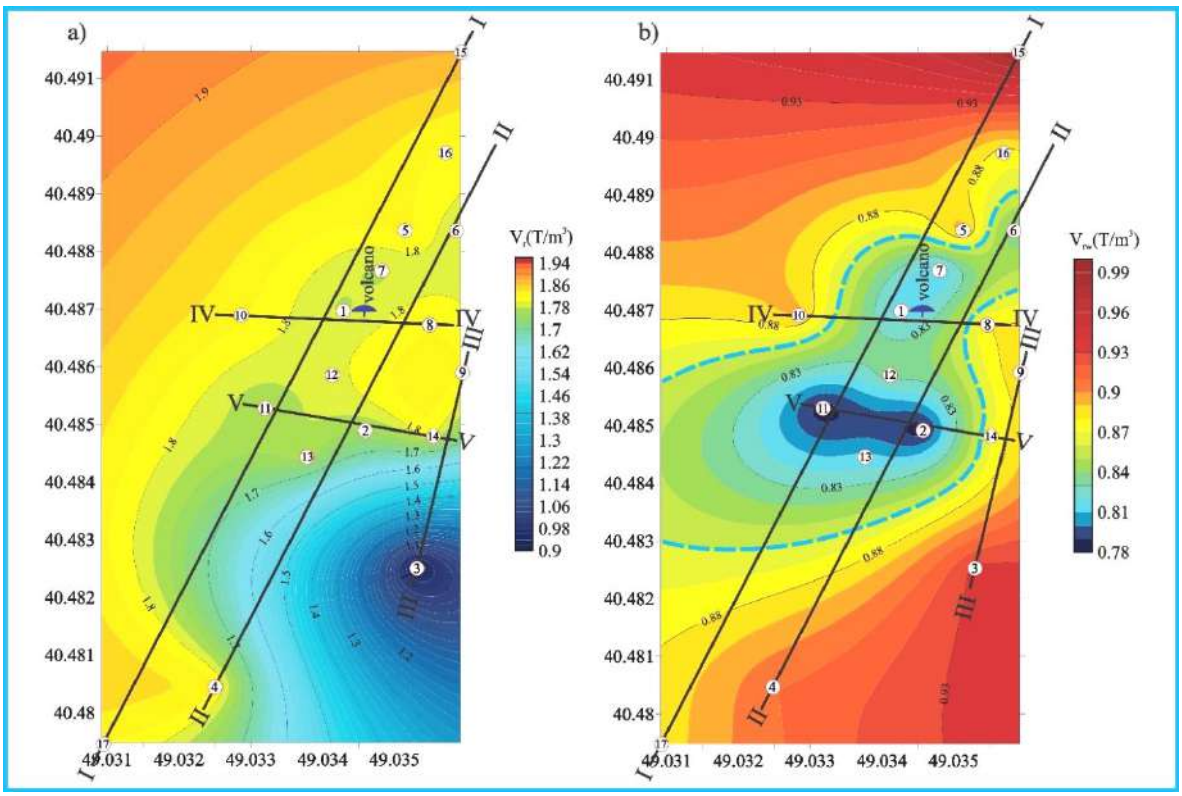

Fig. 9. Maps of the rock densities V_r (a) and V_{rw} (b) compiled using VES data

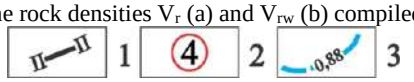

1 – geophysical profiles; 2 – VES points; 3 – 0.88 t/m^3 line

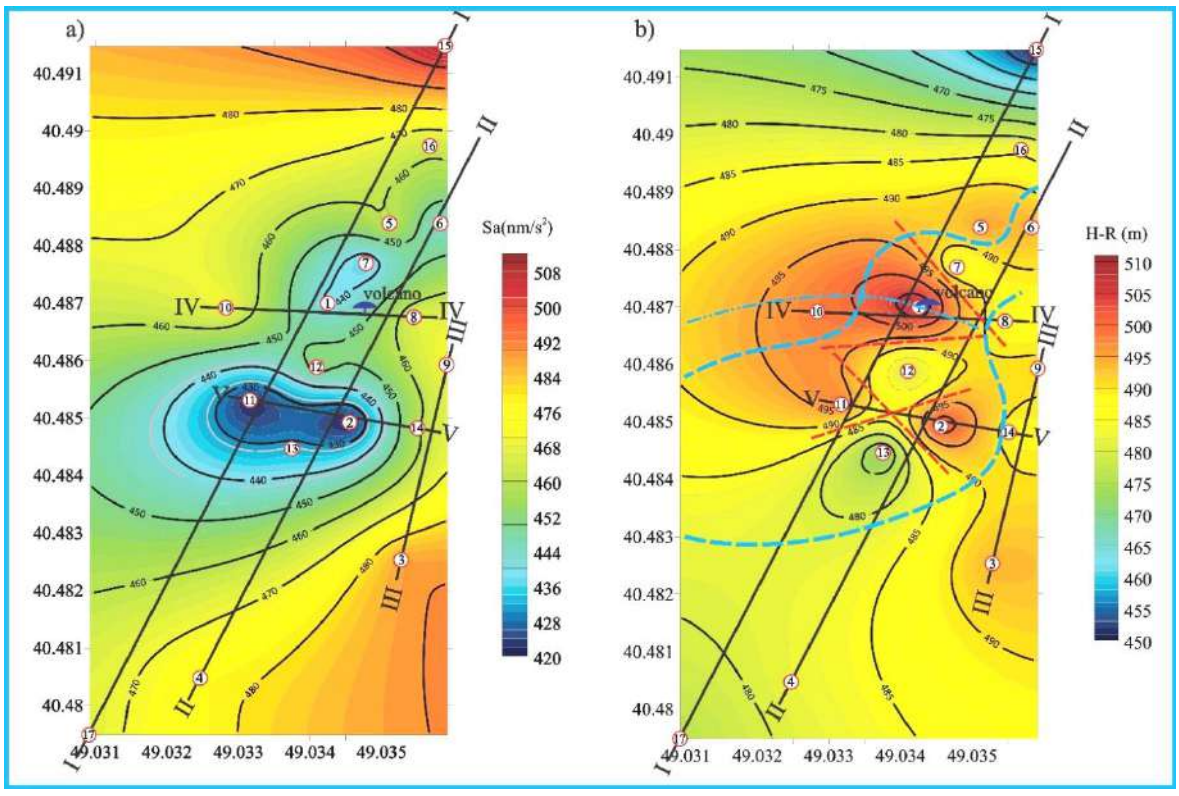

Fig. 10. The maps of seismic acceleration (a) and geophysical survey results (b)

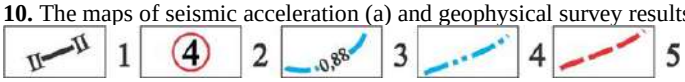

1 – geophysical profile lines; 2 – VES points; 3 – 0.88 t/m^3 lines; 4 – axis of the anti-cline; 5 – supposed faults identified based on the geophysical survey results

Conclusions

Key results of the geophysical survey:

– Detailed dissections of the geological section to a depth of 200 m were conducted;

– Supposed multidirectional faults were identified, presumably formed because of the mud volcano eruption;

– The mud volcano's vent is assumed to dip northeast;

– It was established that the volcano's vent is located in the hinge of an anticline structure;

– It is assumed that the mud volcano is most likely has two vents;

– The main eruption is assumed to have occurred in a marine environment;

– The probable thickness of the volcanic breccia is estimated to be compatible with the depth of the bedrock top, which ranges between 135 and 150 m;

The rocks in the geological section of this area have been found to have relatively high moisture content;

– The density of the rocks in the geological section varies within narrow limits.

It should be noted that the objectives of the geophysical survey were successfully achieved and can be applied to similar problems due to the applied fieldwork methodology.

This work was done by the support of the Oil and Gas Institute, Ministry of Science and Education of the Republic of Azerbaijan.

REFERENCES

Aliyev AdA, Bayramov AA (1999) Some aspects of the tectonics of mud volcanic zones of Gobustan. Proceedings of Azerbaijan Academy of Sciences. The sciences of Earth 1:129–131(in Russian)

Aliyev AdA, Bayramov AA (2000) New data on the features of mud volcanism in the Shamakhi-Gobustan region. Proceedings of geology institute, Azerbaijan Academy of Sciences 28:5–17 (in Russian)

Aliyev AdA, Guliyev IS, Dadashev FG, Rahmanov RR (2015) Atlas of the world mud volcanoes. Publishing house Nafta-Press, Sandro Teti Editore, p 321

Aliyev AdA, Yetirmishli GD (2021) New data on eruptions of mud volcanoes in Azerbaijan. Geology and Geophysics of Russian South 11(2):22–35 (in Russian)

Ali-Zade SA (1987) Anthropocene of Azerbaijan. Elm, Baku, p 244 (in Russian)

Alizadeh AA, Guliyev IS, Kadirov FA, Eppelbaum LV (2016) Geosciences in Azerbaijan, vol 1. Geology. Springer, Heidelberg – N.Y., p 239

Galin DL (1989) Interpretation of engineering geophysics data. Nedra, Moscow, p 114 (in Russian)

Griffiths DH, King RF (1981) Applied geophysics for geologists and engineers: the elements of geophysical prospecting. 2nd edn, Pergamon Press, p 201

Kadirov F, Lerche I, Guliyev I et al (2005) Deep structure model and dynamics of mud volcanoes, Southwest Absheron Peninsula (Azerbaijan). Energy Explor Exploit 23(5):307–332. https://doi.org/10.1260/014459805775992717

Kadirov F, Mammadov S, Reilinger R, McClusky S (2008) Some new data on modern tectonic deformation and active faulting in Azerbaijan (according to Global Positioning System measurements). Proceedings of Azerbaijan Academy of Sciences. The sciences of Earth 1:82–88

Kadirov F, Yetirmishli G, Safarov R et al (2024) Results from 25 years (1998–2022) of crustal deformation monitoring in Azerbaijan and adjacent territory using GPS. ANAS Transaction. Earth Sciences 1:28–43. https://doi.org/10.33677/ggianas20240100107

Kadirov FA, Guliyev IS, Feyzullayev AA et al (2014) GPS-based crustal deformations in Azerbaijan and their influence on seismicity and mud volcanism. Izvestiya, Physics of the Solid Earth, 50:814–823. 6 https://doi.org/10.1134/S1069351314060020

Kadirov FA, Mukhtarov ASh (2004) Geophysical fields, deep structure and dynamics of the Lokbatan Mud Volcano. Izvestiya, Physics of the Solid Earth 40(4):327–333 (in Russian)

Kadirov FA, Safarov RT (2013) Deformation of the Earth's crust of Azerbaijan and adjacent territories based on GPS measurements. Proceedings of Azerbaijan National Academy of Sciences, The Sciences of Earth 1:47–55 (in Russian)

Karakhanyan A, Vernant P, Doerflinger E et al (2013) GPS constraints on continental deformation in the Armenian region and Lesser Caucasus. Tectonophysics 592:39–45. https://doi.org/10.1016/j.tecto.2013.02.002

Keller GV, Frischknecht FC (1966) Electrical methods in Geophysical Prospecting. Pergamon press, New York, reprinted edn, Chapt 3, p 89–180

Khain VE (1984) Regional geotectonics. Alpine Mediterranian belt. Nedra, Moscow, p 344 (in Russian)

Kokh SN, Sokol EV, Dekterev AA et al (2017) The 2011 strong fire eruption of Shikhzarli mud volcano, Azerbaijan: a case study with implications for methane flux estimation. Environ Earth Sci 76(701). https://doi.org/10.1007/s12665-017-7043-5

Lowrıe W (2007) Fundamentals of geophysics. 2nd edn, Cambridge University Press, Swiss Federal Institute of Technology, Zürich, p 381

Milyukov VK, Mironov AP, Rogozhin EA et al (2015) Velocities of contemporary movements of the Northern Caucasus estimated from GPS observations. Geotecton 49:210–218. https://doi.org/10.1134/S0016852115030036

Popov EA, Ten KM, Funtikov GN et al (1990) Guidelines for the use of VES for the detailed dissection of the section in solving geological and engineering-geological problems. Rotaprint, Moscow, p 52 (in Russian)

Raeesi M, Zarifi Z, Nilfouroushan F et al (2017) Quantitative analysis of seismicity in Iran. Pure Appl Geophys 174:793–833. https://doi.org/10.1007/s00024-016-1435-4

Reilinger R, McClusky S, Vernant P et al (2006) GPS constraints on continental deformation in the Africa-Arabia-Eurasia continental collision zone and implications for the dynamics of plate interactions. J Geophys Res 111(BO5411). https://doi.org/10.1029/2005JB004051

Salamov AM, Kadirov AG, Salamov FA, Pashayev TR (2015) Investigation of the landslide in the Khizi region of Azerbaijan by the method of Vertical Electrical Sounding. Inzhenerniye izyskaniya (Engineering survey) 5-6:50–56 (in Russian)

Salamov AM, Mammadov VA, Rashidov TM et al (2023) Electrical resistivity tomography of Lokbatan mud volcano: inner structure and formation mechanism. ANAS Transactions, Earth Sciences 1:49–59. https://doi.org/10.33677/ggianas20230100093

Salamov AM, Safarov RT, Zamanova AH et al (2025) Assessment of exogenıc geologıcal process dynamıcs in the Yanardag area of Absheron peninsula (Azerbaijan) based on Vertıcal Electrıcal Soundıng data, ANAS Transactions. Earth Sciences 2:106–113. https://doi.org/10.33677/ggianas20250200158

Sokhadze G, Floyd M, Godoladze T et al (2018) Active convergence between the Lesser and Greater Caucasus in Georgia: Constraints on the tectonic evolution of the Lesser–Greater Caucasus continental collision. Earth and Planetary Science Letters 481:154–161. https://doi.org/10.1016/j.epsl.2017.10.007

Yakubov AA, Alizade AA, Zeynalov MM (1971) Mud volcanoes of the Azerbaijan SSR. Publishing House of the Academy of Sciences of the Azerbaijan SSR, Baku, p 255 (in Russian)

Yakubovski YuV, Renard IV (1991) Electrical prospecting. Nedra, Moscow, p 347 (in Russian)

ИССЛЕДОВАНИЯ МЕТОДОМ ЭЛЕКТРИЧЕСКОГО СОПРОТИВЛЕНИЯ И ИЗУЧЕНИЕ ПРИПОВЕРХНОСТНОЙ СТРУКТУРЫ ГРЯЗЕВОГО ВУЛКАНА ШЫХЗАХЫРЛИ (АЗЕРБАЙДЖАН)

Кадиров Ф.А.[1,2,3], Саламов А.М.[1], Сафаров Р.Т.[1,2]*, Наджафов О.Ф.[1], Самедли П.М.[2], Мамедов С.Г.[1], Заманова А.Г.[1,2]

[1]Министерство науки и образования Республики Азербайджан, Институт геологии и геофизики, Азербайджан AZ1073, Баку, просп. Г.Джавида, 119

[2]Министерство науки и образования Республики Азербайджан, Институт нефти и газа, Азербайджан AZ1000, Баку, ул. Ф.Амирова, 9

[3]Геологический факультет, Бакинский государственный университет, Азербайджан AZ1148, г. Баку, ул. акад. Захида Халилова, 33

**Автор, отвечающий за переписку: rafiqsafarov@gmail.com*

Резюме. Грязевой вулканизм широко распространен в Азербайджане, на суше и на море насчитывается более 300 грязевых вулканов. Эти вулканы связаны с месторождениями нефти и газа, и многие из них в настоящее время активны. Грязевой вулкан Шыхзахырлы расположен к западу-северо-западу от Баку, в Шамахы-Гобустанской области и является одним из активно действующих грязевых вулканов. С 1844 года по 2025 год произошло около 25 сильных извержений. Последнее извержение вулкана произошло 9 января 2021 года и состояло из трех фаз. Самым продолжительным извержением была третья фаза, длившаяся 7 минут. С целью оценки приповерхностных грязевых камер, а также отслеживания питающего канала в районе грязевого вулкана Шыхзахырлы впервые были проведены геоэлектрические измерения, выполненные методом вертикального электрического зондирования (ВЭЗ). Измерения ВЭЗ показали, что на глубине первых 50 м от поверхности земли не обнаружено неглубоких камер накопления. Извержение, вызванное накоплением газа, в приповерхностном слое, по-видимому, носит разветвленный характер: в одном месте восходящий путь миграции имеет почти вертикальное направление, в других – наклонное. В результате проведенных исследований было установлено, что вулкан, скорее всего, имеет два жерла, расположенных в шарнире антиклинальной структуры. Породы в геологическом разрезе исследуемой области характеризуются относительно высоким содержанием влаги. Предполагаемая толщина вулканической брекчии оценивается как соответствующая глубине залегания верхнего слоя коренных пород, которая колеблется в пределах 135–150 м. Были выявлены предполагаемые системы разломов разного направления, предположительно образовавшиеся в результате извержения грязевого вулкана.

Ключевые слова: *грязевой вулкан, извержение, вертикальное электрическое зондирование, сопротивление, геоэлектрический разрез, Шыхзахырлы, разлом*

ELEKTRİK MÜQAVİMƏTİ MÜŞAHİDƏLƏRİ VƏ ŞIXZAHIRLI PALÇIQ VULKANINDA KİÇİK DƏRİNLİKLƏRDƏ MÖVCUD OLAN STRUKTURLARIN TƏDQİQİ (AZƏRBAYCAN)

Qədirov F.Ə.[1,2,3], Salamov Ə.M.[1], Səfərov R.T.[1,2*], Nəcəfov O.F.[1], Səmədli P.M.[2], Məmmədov S.Q.[1], Zamanova A.H.[1,2]

[1]Azərbaycan Respublikasının Elm və Təhsil Nazirliyi, Geologiya və Geofizika İnstitutu, Azərbaycan AZ1073, Bakı, H.Cavid prosp., 119

[2]Azərbaycan Respublikasının Elm və Təhsil Nazirliyi, Neft və Qaz İnstitutu, Azərbaycan AZ1000, Bakı, F.Əmirov küç., 9

[3]Geologiya Fakültəsi, Bakı Dövlət Universiteti, Azərbaycan AZ1148, Bakı, akad. Zahid Xəlilov küç., 33

**Yazışmalara məsul: rafiqsafarov@gmail.com*

Xülasə. Palçıq vulkanizmi Azərbaycanda geniş yayılmışdır, quruda və dənizdə 300-dən çox palçıq vulkanı mövcuddur. Bu vulkanlar neft və qaz yataqları ilə əlaqəlidir və bir çoxu hazırda aktivdir. Şıxzahırlı palçıq vulkanı Bakının qərb şimal-qərb hissəsində, Şamaxı-Qobustan rayonunda yerləşir və dünyanın aktiv palçıq vulkanlarından biridir. 1844-cü ildən 2025-ci ilə qədər təxminən 25 böyük püskürmə baş vermişdir. Vulkanın son püskürməsi 9 yanvar 2021-ci ildə baş vermiş və üç fazadan ibarət olmuşdur. Ən uzun püskürmə üçüncü fazada baş vermiş və 7 dəqiqə davam etmişdir. Şıxzahırlı palçıq vulkanı ərazisində ilk dəfə olaraq səthə yaxın palçıq kameralarının qiymətləndirilməsi, eləcə də qidalandırıcı kanalın izlənməsi məqsədilə şaquli elektrik zondlama üsulundan (ŞEZ) ibarət geoelektrik ölçmələri aparılmışdır. ŞEZ ölçmələri yer səthindən 50 m altda, kiçik dərinlikdə yığılma kameralarının mövcud olmadığını göstərmişdir. Qaz yığılması ilə tətiklənən püskürmə səthə yaxın bölgədə şaxələnir, bir yerdə yuxarıya doğru miqrasiya yolu demək olar ki, şaquli istiqamətdə olsa da, digər yerlərdə mailidir. Tədqiqatlar nəticəsində müəyyən olunmuşdur ki, vulkanın antiklinal strukturun şarnirində yerləşən çox güman ki, iki boğazı mövcuddur. Tədqiqat sahəsinin geoloji kəsilişindəki süxurların nisbətən yüksək nəmliliyə malik olduğu aşkar edilmişdir. Vulkanik brekçiyanın ehtimal olunan qalınlığının 135-150 m arasında dəyişməklə ana süxurların tavanının dərinliyi ilə uyğun olduğu təxmin edilir. Çox güman ki, palçıq vulkanının püskürməsi nəticəsində əmələ gəlmiş müxtəlif istiqamətli qırılmalar sistemi müəyyən edilmişdir.

Açar sözlər: *palçıq vulkanı, püskürmə, şaquli elektrik zondlama, müqavimət, geoelektrik kəsiliş, Şıxzahırlı, qırılma*